

The Rate of Homolysis of Adducts of Peroxynitrite to the C=O Double Bond

Gábor Merényi,^{*,‡} Johan Lind,[‡] and Sara Goldstein[§]

Contribution from the Department of Chemistry, Nuclear Chemistry, The Royal Institute of Technology, S-10044 Stockholm 70, Sweden, and Department of Physical Chemistry, The Hebrew University of Jerusalem, Jerusalem 91904, Israel

Received July 23, 2001

Abstract: Nucleophilic addition of the peroxynitrite anion, ONOO⁻, to the two prototypical carbonyl compounds, acetaldehyde and acetone, was investigated in the pH interval 7.4–14. The process is initiated by fast equilibration between the reactants and the corresponding tetrahedral adduct anion, the equilibrium being strongly shifted to the reactant side. The adduct anion also undergoes fast protonation by water and added buffers. Consequently, the rate of the bimolecular reaction between ONOO⁻ and the carbonyl is strongly dependent on the pH and on the concentration of the buffer. The pK_a of the carbonyl-ONOO adduct was estimated to be ~11.8 and ~12.3 for acetone and acetaldehyde, respectively. It is shown that both the anionic and the neutral adducts suffer fast homolysis along the weak O–O bond to yield free alkoxy and nitrogen dioxide radicals. The yield of free radicals was determined to be about 15% with both carbonyl compounds at low and high pH, while the remainder collapses to molecular products in the solvent cage. The rate constants for the homolysis of the adducts vary from ca. 3 × 10⁵ to ca. 5 × 10⁶ s⁻¹, suggesting that they cannot act as oxidants in biological systems. This small variation around a mean value of about 10⁶ s⁻¹ suggests that the O–O bond in the adduct is rather insensitive to its protonation state and to the nature of its carbonyl precursor. An overall reaction scheme was proposed, and all the corresponding rate constants were evaluated. Finally, thermokinetic considerations were employed to argue that the formation of dioxirane as an intermediate in the reaction of ONOO⁻ with acetone is an unlikely process.

Introduction

In the recent past, peroxynitrite (ONOOH/ONOO⁻) has acquired a certain notoriety in biological systems.¹ This stems from its facile formation in regions where •NO abounds and formation of O₂•⁻ is favored. Peroxynitrite ion is very stable, but it decomposes upon protonation by homolysing along the weak O–O bond,² yielding about 28% •OH and •NO₂ free radicals,^{3,4} while the remainder collapses to nitric acid in the solvent cage. ONOO⁻ reacts relatively fast with CO₂, i.e., $k = (2.9 \pm 0.3) \times 10^4 \text{ M}^{-1} \text{ s}^{-1}$ at 24 °C,⁵ and therefore in biological systems, where high concentrations of CO₂ prevail, most peroxynitrite is scavenged by it. This reaction presumably forms an adduct to one of the two C=O bonds of CO₂. For all intents and purposes this adduct behaves like ONOOH itself; i.e., ONOOC(O)O⁻ homolyzes to yield about 33% •NO₂ and CO₃•⁻ free radicals,^{4,6–9} and the remainder forms NO₃⁻ and CO₂ in

the solvent cage. However, the lifetime of the adduct is not known apart from an experimentally derived upper limit of 2–3 ms.^{9,10} Nevertheless, both quantum-chemical calculations¹¹ and thermokinetic estimations¹² concur that a substantial weakening of the O–O bond occurs in ONOOC(O)O⁻ as compared to the bond strength in ONOOH. Peroxynitrite ion has also been shown to react with other carbonyl compounds, such as aldehydes^{4,13,14} and ketones.^{15,16} The same reactivity pattern was derived for aldehydes as for CO₂, namely adduct formation followed by O–O homolysis. The yields of free radicals in this case, i.e., •NO₂ and alkoxy radicals, vary between 10 and 40%.^{4,14} However, in the case of ketones this obvious pattern was considered a minor reaction at best, and a heterolytic mechanism involving a dioxirane intermediate was proposed as the main pathway.¹⁵ There can be no doubt that addition of ONOO⁻ to carbonyl compounds complies with the well-established pattern of nucleophilic addition. The latter has been extensively explored in several processes, e.g., ester hydrolysis, and the whole

* To whom correspondence should be addressed.

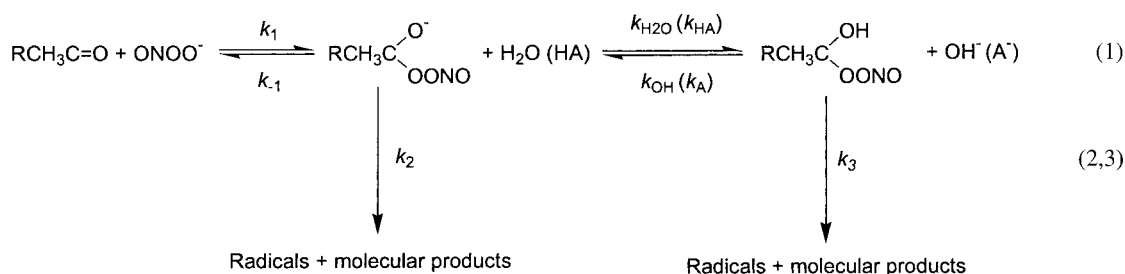
‡ The Royal Institute of Technology.

§ The Hebrew University of Jerusalem.

- (1) Marnett, L. J. *Chem. Res. Toxicol.* **1998**, *11*, 709–721.
- (2) Mahoney, L. R. *J. Am. Chem. Soc.* **1970**, *92*, 5262–5263.
- (3) Gerasimov, O. V.; Lymar, S. V. *Inorg. Chem.* **1999**, *38*, 4317–4321.
- (4) Hodges, G. R.; Ingold, K. U. *J. Am. Chem. Soc.* **1999**, *121*, 10695–10701.
- (5) Lymar, S. V.; Hurst, J. K. *J. Am. Chem. Soc.* **1995**, *117*, 8867–8868.
- (6) Lymar, S. V.; Hurst, J. K. *Inorg. Chem.* **1998**, *37*, 294–301.
- (7) Goldstein, S.; Czapski, G. *Inorg. Chem.* **1997**, *36*, 5113–5117.
- (8) Goldstein, S.; Czapski, G. *J. Am. Chem. Soc.* **1998**, *120*, 3458–3463.
- (9) Goldstein, S.; Czapski, G.; Lind J.; Merényi, G. *Chem. Res. Toxicol.* **2001**, *14*, 1273–1276.

- (10) Lymar, S. V.; Jiang, Q.; Hurst, J. K. *Biochemistry* **1996**, *35*, 7855–7861.
- (11) Houk, K. N.; Condroski, K. R.; Pryor, W. A. *J. Am. Chem. Soc.* **1996**, *118*, 13002–13006.
- (12) Merényi, G.; Lind, J. *Chem. Res. Toxicol.* **1997**, *10*, 1216–1220.
- (13) Uppu, R. M.; Winston, G. W.; Pryor, W. A. *Chem. Res. Toxicol.* **1997**, *10*, 1331–1337.
- (14) Nakao, L. S.; Ouchi, D.; Augusto, O. *Chem. Res. Toxicol.* **1999**, *12*, 1010–1018.
- (15) Yang, D.; Tang, Y.-C.; Chen, J.; Wang, X.-C.; Bartberger, M. D.; Houk, K. N.; Olson, L. *J. Am. Chem. Soc.* **1999**, *121*, 11976–11983.
- (16) Tibi, S.; Koppenol, W. H. *Helv. Chim. Acta.* **2000**, *83*, 2412–2424.

Scheme 1



impressive armament of physical organic chemistry has been brought to bear on these biologically vital reactions.¹⁷ In Scheme 1 the various reactions are given in the case where ONOO⁻ is the nucleophile. The only feature in Scheme 1 which is unique to ONOO⁻ as the nucleophile is that its adduct (unlike the OH⁻ adduct) can undergo homolysis.

The peroxynitrite adduct to CO₂ is a carboxylate ion, and therefore the pK_a of ONOOC(O)OH must be far below pK_a(ONOOH) = 6.6,¹⁸ which eliminates the effect of acid/base catalysis. On the other hand, the peroxynitrite adducts to aldehydes and ketones are hemiacetals and ketals, respectively, with pK_a > 10.¹⁹ Therefore, the combined effects of acid/base and buffer catalysis can be utilized to extract mechanistic details. Specifically, as occurred to us in the case of acetone and acetaldehyde, a competition between protonation/deprotonation and homolysis of the carbonyl-ONOO adduct can reveal the rate of this latter, normally elusive reaction. The present work will delve into the detailed mechanism of nucleophilic addition of ONOO⁻ to acetaldehyde and acetone, two prototypical carbonyl compounds. These systems will be studied at pH > pK_a(ONOOH) since it has already been shown that the acid, ONOOH, is much less reactive than the base, ONOO⁻, toward carbonyl groups,^{15,16} a well-known behavior with other nucleophiles.

Experimental Section

Chemicals. All chemicals were of analytical grade and were used as received. Solutions were prepared with distilled water, which was further purified using a Milli-Q water purification system. Fresh solutions of ONOO⁻ were prepared daily by reacting nitrite with acidified hydrogen peroxide using a quenched flow with a computerized syringe pump (World Precision Instruments model SP 230IW), as described elsewhere.²⁰ Briefly, 0.63 M nitrite was mixed with 0.60 M H₂O₂ in 0.70 M HClO₄, and the mixture was quenched with 3 M NaOH at room temperature. The yield of ONOO⁻ was determined from its absorption at 302 nm using $\epsilon = 1670 \text{ M}^{-1}\text{cm}^{-1}$.²¹ The stock solution contained 0.12 M ONOO⁻, 0.767 M NaOH, 10 mM nitrite, and practically no residual H₂O₂. ONOO⁻ was diluted in 1×10^{-4} –1 M NaOH solutions, which were prepared from 1.0 N sodium hydroxide (BDH).

The yield of acetate produced in the reaction of ONOO⁻ with acetone in strongly basic acetone solutions was determined using gas chromatography. The analyses were conducted on a Philips PYE UNICAM series 304 GC with a flame ionization detector (FID). A Supelco WAX column (internal diameter 0.25 μm , film thickness 0.25 μm , and length 30 m) was used with temperature programming (60 °C (0.5 min), 15

°C min⁻¹ until 220 °C (5 min)) and helium as the carrier gas at a pressure of 1.3 bar. Identification of the compounds was made by comparison of retention times with those of authentic reference samples. For quantitative determination of acetic acid, a known amount of benzothiazole was used as an internal standard. Briefly, 5-mL amounts of 30–40 mM ONOO⁻ solutions in 5 M NaOH were mixed with 2 mL of 2.5 M acetone in 2 M NaOH. After sufficient reaction time, 0.5 mL of concentrated sulfuric acid was added to acidify the solution, and the resulting mixture was injected into the GC.

Apparatus. Stopped-flow kinetic measurements were carried out using the Bio SX-17MV sequential stopped flow from Applied Photophysics coupled with a 1-cm-long mixing cell. Alkaline solutions of ONOO⁻ were mixed in a 1:1 ratio with the carbonyl compounds dissolved in water in the absence and in the presence of ammonia or phosphate buffers. The decomposition of ONOO⁻ was followed at 302 or 320–340 nm in the presence of relatively high concentrations of acetone and NH₄NO₃. In some experiments ferrocyanide and tetranitromethane (TNM) were added, and the formation of ferricyanide and C(NO₂)₃⁻ was followed at 420 nm ($\epsilon = 1000 \text{ M}^{-1} \text{ s}^{-1}$) and 350 nm ($\epsilon = 14\,400 \text{ M}^{-1} \text{ s}^{-1}$), respectively. Each experiment was done at least three times, and the average value is given. The pH of the mixture was measured at the outlet of the flow system. The limit errors were in most cases less than 3%. In the presence of relatively high concentrations of NH₄⁺, the experimental error was ca. 10% due to the Schlieren effect but diminished at low concentrations of NH₄⁺, i.e., when the solution became homogeneous. All experiments were carried out at 22 °C.

Pulse radiolysis experiments were carried out with a Varian 7715 linear accelerator with 5-MeV electron pulses of 1.5 μs and 200 mA. All measurements were made at room temperature in a 4-cm Spectroil cell using three light passes (optical path length 12.1 cm).

Modeling of the experimental results was carried out using INTKIN, a noncommercial program developed at Brookhaven National Laboratories by Dr. H. A. Schwarz.

Results

The Effect of pH and Buffers. The reaction of ONOO⁻ with acetone and acetaldehyde was studied under limiting concentration of ONOO⁻, and the rate of decay of ONOO⁻ was found to be linearly dependent on the carbonyl concentration (results not shown). In the case of acetaldehyde, the decay of the absorption followed two sequential first-order reactions. The observed first-order rate constant of the first decay was linearly dependent on the concentration of CH₃CHO, and that of the second decay was determined to be $0.8 \pm 0.2 \text{ s}^{-1}$ under all our experimental conditions. The second process is attributed to the decay of O₂NOO⁻, which is known to form via the reaction of ONOO⁻ with aldehydes.⁴ The rate of reaction of ONOO⁻ with these carbonyls increased upon decreasing the pH. Aldehydes and ketones in aqueous solutions exist in equilibrium between free and hydrated forms,²² where the nucleophilic addition of ONOO⁻ occurs only to the free form. The concentration of the free form also depends on the pK_a of the hydrated forms, which

(17) (a) Johnson, S. L. In *Advances in Physical Organic Chemistry*; Gold, V., Ed.; Academic Press: London, 1967; Vol. 5, pp 237–330. (b) Jencks, W. P. *Acc. Chem. Res.* **1980**, *13*, 161–169.

(18) Logager, T.; Sehested, K. *J. Phys. Chem.* **1993**, *97*, 6664–6669.

(19) Sander, E. G.; Jencks, W. P. *J. Am. Chem. Soc.* **1968**, *90*, 6154–6162.

(20) Saha, A.; Goldstein, S.; Cabelli, D.; Czapski, G. *Free Rad. Biol. Med.* **1998**, *23*, 653–659.

(21) Hughes, M. N.; Nicklin, H. G. *J. Chem. Soc. (A)* **1968**, 450–452.

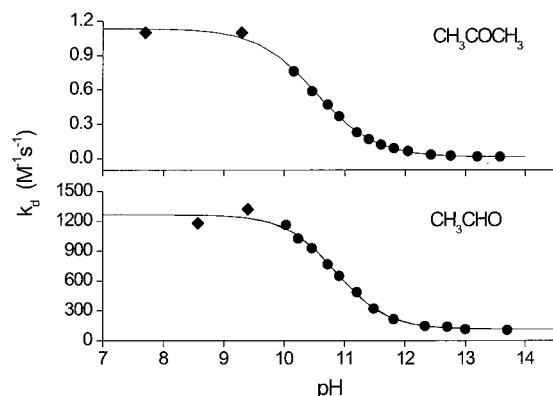


Figure 1. Rate of the reaction of ONOO^- with acetone and acetaldehyde as a function of pH in the absence (●) and in the presence (◆) of low concentrations of buffers. The solid lines are sigmoidal fits to the data. The asymptote values for acetone are 0.014 ± 0.003 and $1.14 \pm 0.02 \text{ M}^{-1} \text{ s}^{-1}$, and the center is at $\text{pH } 10.5 \pm 0.1$. The asymptote values for acetaldehyde are $(1.15 \pm 0.23) \times 10^2$ and $(1.27 \pm 0.04) \times 10^3 \text{ M}^{-1} \text{ s}^{-1}$, and the center is at $\text{pH } 10.9 \pm 0.1$.

Table 1. Effect of Phosphate Buffer Concentration on the Observed Rate Constant of the Reaction of 24–270 μM ONOO^- with 0.068 M Acetone or 6.6 mM Acetaldehyde

[phosphate] ₀ , M	pH	k_{obs} , s^{-1}	
		acetaldehyde	acetone
1.5	7.6, 7.7	13.8	1.5
0.75	7.5, 7.7	12.3	0.65
0.38	7.4, 7.7	8.5	0.44
0.19	7.4, 7.7	5.6	0.30
0.094	7.5, 7.7	4.4	0.23
0.038	7.6, 7.6	3.6	
0.023	7.8		0.18
0.015	7.9, 7.7	3.4	0.18
0.011	7.7		0.17
0.0078	7.8		0.17
0.0075	8.1	3.2	
0.0075	8.6	3.3	

is usually above 13. The hydrated form in the case of acetone is only about 0.2%, and it was therefore ignored. In the case of acetaldehyde the hydrate/free aldehyde ratio is 1.4,²² the pK_a of the hydrated form is 13.6,²² and therefore the ratio of deprotonated to neutral aldehyde hydrate is $2.7[\text{OH}^-]$. Thus, the bimolecular rate constants for the reaction of ONOO^- with acetaldehyde and acetone were calculated to be $k_d = k_{\text{obs}}\{1 + 1.4(1 + 2.7[\text{OH}^-])\}/[\text{CH}_3\text{CHO}]_0$ and $k_d = k_{\text{obs}}/[\text{CH}_3\text{COCH}_3]_0$, where the initial concentration is that of the total carbonyl compound. These k_d values were plotted as a function of the pH in Figure 1. Clearly, buffers have to be added at $\text{pH} < 11$ to maintain a constant pH, and as can be seen from Tables 1 and 2, k_d is also strongly dependent on the concentrations of phosphate or ammonium buffers. To obtain accurate values for k_d without the interference of buffer catalysis, k_d was plotted against [buffer] at relatively low buffer concentrations. One such plot is shown in Figure 2 (lower curve). We note that the contribution of the self-decomposition of ONOO^- to the observed rate constant could not be ignored in the case of acetone in phosphate buffer. In this case, $k_d = (k_{\text{obs}} - k_0)/[\text{CH}_3\text{COCH}_3]_0$, where k_0 was determined to be 0.11 s^{-1} at $\text{pH } 7.7$ (15 mM phosphate buffer). The buffer-independent k_d values were extracted from the intercepts of these straight lines and

Table 2. Effect of $[\text{NH}_4^+]$ on k_d Obtained in the Reaction of 15–430 μM ONOO^- with 0.068–0.1 M Acetone or 1.1–8.4 mM Acetaldehyde

$[\text{NH}_4^+]_0$, M	pH	$[\text{NH}_4^+]$, M^a	k_d , $\text{M}^{-1} \text{ s}^{-1b}$	
			acetaldehyde	acetone
5.0	7.9	5.0		1.0×10^2
3.25	7.9	3.25	4.2×10^4	
2.5	7.9	2.5	4.4×10^4	94
1.62	7.7	1.63	3.7×10^4	
1.25	7.8	1.25	3.9×10^4	76
0.98	7.7	0.98	2.9×10^4	
0.63	8.0	0.63	2.3×10^4	51
0.5	7.7	0.5	2.1×10^4	
0.31	7.9	0.31	1.5×10^4	36
0.25	7.8	0.25	1.4×10^4	
0.16	8.0	0.16	1.1×10^4	
0.13	8.0	0.13		21
0.10	7.9	0.10	9.1×10^3	
0.078	8.1	0.073	7.8×10^3	
0.05	8.2	0.045	7.3×10^3	12
0.025	8.4	0.022	5.0×10^3	6.3
0.018	8.5	0.0077	2.5×10^3	
0.01	8.8	0.0074		3.3
0.005	9.0	0.0033	2.2×10^3	
0.004	9.25	0.002		1.8
0.0036	8.9	0.0025	1.5×10^3	
0.0012	9.37	5.2×10^{-4}		1.4
0.001	9.3	4.7×10^{-4}	1.4×10^3	
5.4×10^{-4}	9.31	1.6×10^{-4}		1.2
5.0×10^{-4}	9.4	2.0×10^{-4}	1.3×10^3	
1.7×10^{-4}	9.45	6.5×10^{-5}		1.1

^a The concentration of NH_4^+ was calculated using $\text{pK}_a = 9.25$ ($I = 0$), 9.3 ($I = 0.1$ –0.5 M), 9.4 ($I = 1$ M), 9.49 ($I = 2$ M), and 9.8 ($I = 5$ M).
^b The contribution of the self-decomposition of peroxyxynitrite was ignored.

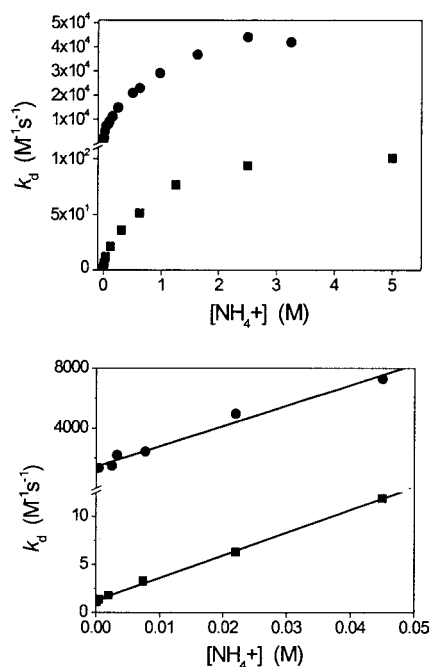


Figure 2. Plots of k_d vs $[\text{NH}_4^+]$ at high (upper) and low (lower) buffer concentrations for acetone (■) and acetaldehyde (●). Data were taken from Table 2.

are included in Figure 1. Although the k_d values for acetaldehyde are significantly higher than those for acetone at all pH's, both compounds display similar pH profiles, possessing an upper limiting value at low pH and a lower limiting value at very high pH. The pH intervals in which the transition from high to low limiting k_d occurs are also similar for both compounds. The

(22) Bell, R. P. In *Advances in Physical Organic Chemistry*; Gold, V., Ed.; Academic Press: London, 1966; Vol. 4, pp 1–29.

Table 3. Yields of Ferricyanide Obtained in the Reaction of ONOO⁻ with Acetone and Acetaldehyde

[Fe(CN) ₆ ⁴⁻], mM	[Fe(CN) ₆ ³⁻]/[ONOO ⁻], %	
	acetone ^a	acetaldehyde ^d
100	28.1	20.6, ^b 20.1 ^c
50	27.3	16.6, ^b 19.8 ^c
20		16.4 ^c
12.5	22.5	
5		10.9, ^b 15.4 ^c
2.5	15.3	
2		12.5 ^c
1	12.1	6.6 ^b
0.9		6.8 ^c
0.5	10.1	5.7 ^b
0.4		4.1 ^c

^a The reaction of 0.32 mM ONOO⁻ with 0.2 M acetone was studied in the presence of 0.6 M ammonium buffer at pH 8.8–9.0. ^b The reaction of 0.38 mM ONOO⁻ with 5 mM acetaldehyde was studied in the presence of 0.1 M ammonium buffer at pH 8.8. ^c The reaction of 0.38 mM ONOO⁻ with 21 mM acetaldehyde was studied in the presence of 0.1 M NaOH. ^d The formation of ferricyanide at low concentrations of ferrocyanide, i.e., [Fe(CN)₆⁴⁻] < 10 mM, followed two sequential first-order reactions, and the yields are the sum obtained in these two processes. The contribution of the second process did not exceed 2%.

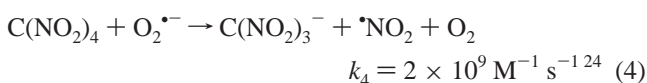
data in Figure 1 were fitted to sigmoidal curves, which resulted in two plateau values, 0.014 ± 0.003 and 1.14 ± 0.02 M⁻¹ s⁻¹ for acetone, and 115 ± 25 and (1.27 ± 0.04) × 10³ M⁻¹ s⁻¹ for acetaldehyde. Similarly, the apparent pK_s's for the transition between the two plateaus are 10.5 ± 0.1 and 10.9 ± 0.1 for acetone and acetaldehyde, respectively.

Product Yields. The yields of the oxidizing intermediates formed in the reaction of ONOO⁻ with acetaldehyde were determined at pH 8.8 and pH 13 using ferrocyanide as a scavenger. The yields of ferricyanide obtained in the presence of various concentrations of ferrocyanide are given in Table 3. The formation of ferricyanide at low concentrations of ferrocyanide followed two sequential first-order reactions, and the yields given in Table 3 are the sums of these two processes. The contribution of the slow process to the total yield was less than 2%.

In the case of acetone, the yield of the oxidizing intermediates at high pH could not be measured because relatively high concentrations of acetone are required to compete efficiently with the homolysis of ONOO⁻ into •NO and O₂^{•-} (*k* = 0.017 s⁻¹),²³ and under these conditions ferrocyanide is insoluble. Therefore, we determined the yield of the oxidizing intermediates at pH 8.9–9, using relatively high concentrations of ammonium buffer and acetone. The results are summarized in Table 3.

The yield of acetate has already been measured in the case of acetaldehyde at pH 6.7 and 9.1.¹⁴ In the present study we determined its yield in the acetone system in the presence of 1–2 M NaOH to be 13 ± 2%.

The yield of O₂^{•-} formed as an intermediate in the reaction of 96–335 μM ONOO⁻ with 0.1 M acetone in the presence of 0.1 M NH₄⁺ (pH 8.0) was determined by adding 63–418 μM TNM.

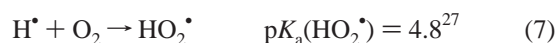
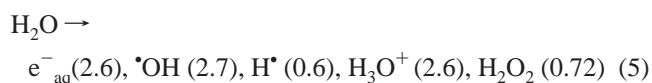


Under these conditions ONOO⁻ decayed in the absence of TNM with *k* = 1.7 ± 0.1 s⁻¹. When TNM was included, the formation

of C(NO₂)₃⁻ followed two sequential first-order reactions with *k*(1) = 1.8 ± 0.1 s⁻¹, practically the same as in the absence of TNM, and *k*(2) = 0.015 ± 0.001 s⁻¹, respectively. The yields of C(NO₂)₃⁻ per [ONOO⁻]₀, which are the same as those of O₂^{•-}, were determined to be 2.0 ± 0.3% in the fast process and 3.1 ± 0.2% in the slow process. Since the rate constant for the homolysis of ONOO⁻ into •NO and O₂^{•-} is 0.017 s⁻¹,²³ we calculate that (0.017/1.7) × 100 = 1.0% O₂^{•-} must derive from this homolysis reaction. Thus, the reaction of ONOO⁻ with acetone forms in total ~2 + 3 – 1 = 4% O₂^{•-}, out of which about 1% is formed at the same rate as ONOO⁻ decomposes, and the rest is produced in a subsequent relatively slow process.

The yield of O₂NOO⁻ (ε₂₈₅ = 1550 M⁻¹ cm⁻¹)²⁵ formed in the reaction of ONOO⁻ with acetaldehyde was determined at pH 13 and pH 7.7–8.1 (0.2 M phosphate or 0.1 M ammonia) to be 10.9 ± 1.1% and 8.7 ± 0.4%, respectively.

The Decomposition of CH₃OO•. CH₃OO• has already been shown to form as an intermediate in the reaction of ONOO⁻ with acetaldehyde,¹⁴ and we will show below that it also forms in the acetone system. Therefore, it was essential to verify the single literature value²⁶ cited for the rate of self-decomposition of this radical, i.e., 2*k* = 8 × 10⁸ M⁻¹ s⁻¹, and to determine the yield of O₂^{•-} formed in this process. CH₃OO• was generated upon irradiation of aqueous solutions saturated with N₂O/O₂ (4:1), which contained 50 mM dimethyl sulfoxide (DMSO), 5 μM diethylenetriaminepentaacetic acid (DTPA), and 3 mM phosphate buffer at pH 7.6. DTPA was added to avoid catalysis of O₂^{•-} decomposition by traces of metal impurities. Under these conditions the following reactions take place (given in parentheses are the radiation–chemical yields of the species, defined as the number of species produced by 100 eV of energy absorbed):



The formation and decay of the absorption was followed at 255 nm using 6.2 Gy/pulse. The absorption formed immediately after the pulse is the sum of about 90% CH₃OO• and 10% O₂^{•-} (ε₂₅₅ = 2050 M⁻¹ cm⁻¹),²⁷ and the extinction coefficient of CH₃OO• was calculated to be 1580 ± 150 M⁻¹ cm⁻¹. The decay of the absorbance followed second-order kinetics with 2*k* = (7.3 ± 1.9) × 10⁸ M⁻¹ s⁻¹, in excellent agreement with the literature value obtained using flash photolysis.²⁶

The yield of O₂^{•-} formed during the self-decomposition of CH₃OO• was determined using 0.1 mM TNM in solutions

(23) Merényi, G.; Lind, J. *Chem. Res. Toxicol.* **1998**, *11*, 243–246.

(24) Rabani, J.; Mulac, W. A.; Matheson, M. S. *J. Phys. Chem.* **1965**, *69*, 53.

(25) Goldstein, S.; Czapski, G.; Lind, J.; Merényi, G. *Inorg. Chem.* **1998**, *37*, 3943–3947.

(26) Nikolaev, A. I.; Safiullin, R. L.; Enikeeva, L. R.; Komissarov, U. D. *Khim. Fiz.* **1992**, *11*, 69–72.

(27) Bielski, B. H. J.; Cabelli, D. E.; Arudi, R. L.; Ross, A. B. *J. Phys. Chem. Ref. Data* **1985**, *14*, 1041–1100.

saturated with $\text{N}_2\text{O}/\text{O}_2$ (9:1), which also contained 0.3 M DMSO and 30 mM phosphate buffer at pH 7.6. The yield of $\text{O}_2^{\bullet-}$ formed via the self-decomposition of $\text{CH}_3\text{OO}^\bullet$ was calculated according to eq 10 to be $29 \pm 3\%$ of the initial concentration of $\text{CH}_3\text{OO}^\bullet$, where $[\text{radical}]_{\text{pulse}}$ is the initial concentration of the radicals, i.e., $[\text{CH}_3\text{OO}^\bullet]_{\text{pulse}}/[\text{O}_2^{\bullet-}]_{\text{pulse}} \approx 9$ and $[\text{CH}_3\text{OO}^\bullet]_{\text{pulse}} = 3.7 \mu\text{M}$.

$$\frac{[\text{O}_2^{\bullet-}]}{[\text{CH}_3\text{OO}^\bullet]_0} = \frac{[\text{C}(\text{NO}_2)_3^-]_{\text{exp}} - [\text{O}_2^{\bullet-}]_{\text{pulse}}}{[\text{CH}_3\text{OO}^\bullet]_{\text{pulse}} - [\text{C}(\text{NO}_2)_3^-]_{\text{exp}}} \quad (10)$$

This calculation took into account the initial formation of 10% $\text{O}_2^{\bullet-}$ by the pulse (reaction 7) and the fast reaction of $\text{CH}_3\text{OO}^\bullet$ with $\bullet\text{NO}_2$ (see below), where the latter is formed via reaction 4. As will be shown below, the stability of CH_3OONO_2 is similar to that of HOONO_2 .²⁸ Therefore, it should be stable within the time scale of $\text{CH}_3\text{OO}^\bullet$ decomposition. Consequently, its formation reduces the amount of $\text{CH}_3\text{OO}^\bullet$ that undergoes self-recombination.

The rate constant for the reaction of $\text{CH}_3\text{OO}^\bullet$ with $\text{Fe}(\text{CN})_6^{4-}$ was determined by following the formation of $\text{Fe}(\text{CN})_6^{3-}$ at 420 nm in solutions saturated with $\text{N}_2\text{O}/\text{O}_2$ (4:1), which contained 1.4 M DMSO, 0.05–0.2 M $\text{Fe}(\text{CN})_6^{4-}$, and 3 mM phosphate buffer (pH 7.5). Under these conditions DMSO competes efficiently with $\text{Fe}(\text{CN})_6^{4-}$ for the hydroxyl radical. The buildup of the absorption obeyed first-order kinetics, but k_{obs} vs $[\text{Fe}(\text{CN})_6^{4-}]$ resulted in a relatively large intercept due to the contribution of the radical–radical reaction to the rate. From the slope of such a plot we determined the rate for the reaction of $\text{CH}_3\text{OO}^\bullet$ with $\text{Fe}(\text{CN})_6^{4-}$ to be $(7.1 \pm 1.2) \times 10^3 \text{ M}^{-1} \text{ s}^{-1}$, in excellent agreement with an earlier determination at pH 13.²⁹

Discussion

The Decomposition of ONOO^- in the Presence of Carbonyls. The mechanism of the reaction of ONOO^- with carbonyls is described in Scheme 1. According to this model, and assuming the steady-state approximation for $\text{R}_1\text{R}_2\text{C}(\text{O}^-)$ (ONOO^-) and $\text{R}_1\text{R}_2\text{C}(\text{OH})(\text{ONOO}^-)$, rate equation 11 is obtained, where $\alpha = k_3/(k_{\text{OH}}[\text{OH}^-] + k_3)$.

$$-\frac{d[\text{ONOO}^-]}{dt} = \frac{k_1(\alpha k_{\text{H}_2\text{O}} + k_2)}{(k_{-1} + \alpha k_{\text{H}_2\text{O}} + k_2)} [\text{R}_1\text{R}_2\text{C}=\text{O}] \times [\text{ONOO}^-] = k_d [\text{R}_1\text{R}_2\text{C}=\text{O}] [\text{ONOO}^-] \quad (11)$$

At low pH, $\alpha = 1$ and $k_d = k_1(k_{\text{H}_2\text{O}} + k_2)/(k_{-1} + k_{\text{H}_2\text{O}} + k_2)$. At high pH, $\alpha k_{\text{H}_2\text{O}}$ can be ignored, and $k_d = k_1 k_2/(k_{-1} + k_2)$. Thus, k_d approaches two plateau values at low and high pH, as can be seen in Figure 1. Since the plateau value at low pH exceeds that at high pH, it follows that $k_{-1} > k_2$ and $k_{\text{H}_2\text{O}} > k_2$. Furthermore, since k_d strongly depends on the buffer concentration, k_{-1} must be significantly higher than $k_{\text{H}_2\text{O}}$, i.e., $k_{-1} > k_{\text{H}_2\text{O}} > k_2$. Therefore, to a good approximation, k_d is equal to $K_1 k_2$ at high pH and to $K_1 k_{\text{H}_2\text{O}}$ at low pH.

In the intermediate region we have $k_d \approx K_1 \alpha k_{\text{H}_2\text{O}} + K_1 k_2$. We can easily identify the two terms on the right-hand side of this equation. The second term is the rate constant with which

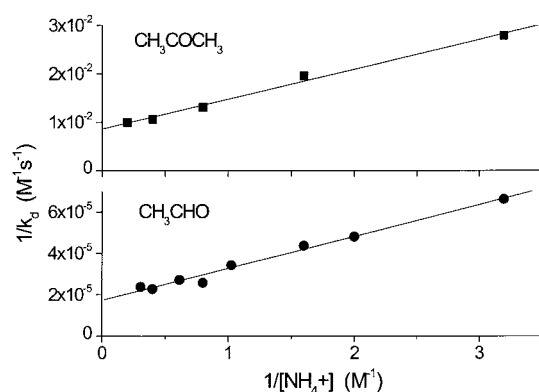


Figure 3. Double reciprocal plots of k_d vs $[\text{NH}_4^+]$. Data were taken from Table 2. The linear fits to the data result for acetone in an intercept = $(8.6 \pm 0.5) \times 10^{-3} \text{ M s}$ and a slope = $(6.2 \pm 0.3) \times 10^{-3} \text{ M}^2 \text{ s}$, and for acetaldehyde an intercept = $(1.7 \pm 0.1) \times 10^{-5} \text{ M s}$ and a slope = $(1.5 \pm 0.1) \times 10^{-5} \text{ M}^2 \text{ s}$.

products are formed via the decomposition of the deprotonated adduct, i.e., via reaction 2, which is constant throughout the whole pH region. The first term, in turn, describes the rate constant with which products are formed via the neutral adduct channel, i.e., reaction 3, which varies from zero at very high $[\text{OH}^-]$ to the low pH plateau value, $K_1 k_{\text{H}_2\text{O}}$. In Figure 1, $\alpha = 1/2$ at the apparent pK, and at this pH, $k_{\text{OH}}[\text{OH}^-] = k_3$; i.e., the neutral adduct is deprotonated by OH^- at the same rate as it decomposes to products.

In the presence of a buffer k_d is given by eq 12, where $\beta = k_3/(k_3 + k_{\text{A}}[\text{A}^-])$.

$$k_d = k_1(\beta(k_{\text{H}_2\text{O}} + k_{\text{HA}}[\text{AH}]) + k_2) / (k_{-1} + \beta(k_{\text{H}_2\text{O}} + k_{\text{HA}}[\text{AH}]) + k_2) \quad (12)$$

At low $[\text{AH}]$, $\beta = 1$, $k_d = K_1 k_{\text{H}_2\text{O}}$, and one should obtain the low pH plateau value at low buffer concentrations. An example of this is seen in the lower curve of Figure 2 (see also Tables 1, 2).

In the presence of high $[\text{AH}]$, k_d approaches k_1 , and therefore a curvature should be observed in plots of k_d vs $[\text{HA}]$. In Figure 2 (upper curve) such curvatures and the approach of k_d toward an upper limit are clearly observed with ammonium buffer for both acetaldehyde and acetone (see also Table 2). These findings reveal that the role of the buffer acid is to protonate the adduct anion, in accordance with Scheme 1. Similarly, the curvature of k_d in Figure 2a is incompatible with an earlier suggestion,¹⁵ according to which a general acid-catalyzed ONOO^- addition to the carbonyl compound is the rate-determining step. Clearly, the latter model would demand k_d to increase linearly with $[\text{buffer}]$ at all concentrations.

At high $[\text{AH}]$ eq 13 is obtained, and assuming $\beta \approx 1$, plots of $1/k_d$ vs $1/[\text{NH}_4^+]$ should yield straight lines with $1/\text{intercept} = k_1$ and slope/intercept = k_{-1}/k_{HA} .

$$k_d = k_1 \beta k_{\text{HA}} [\text{AH}] / (k_{-1} + \beta k_{\text{HA}} [\text{AH}]) \quad (13)$$

Such inverse plots are given in Figure 3 (the data are taken from Table 2). The excellent linearity of the plots confirms the above model and is consistent with β being close to 1. From the intercepts of these plots one obtains $k_1 = 116 \pm 7$ and $(5.8 \pm 0.4) \times 10^4 \text{ M}^{-1} \text{ s}^{-1}$ for acetone and acetaldehyde, respectively. These values, which are the only absolute rate constants

(28) Régimbal, J.-M.; Mozurkewich, M. *J. Phys. Chem. A* **1997**, *101*, 8822–8829.

(29) Das, T. N.; Dhanasekaran, Z. B.; Alfassi, Z. B.; Neta, P. *J. Phys. Chem. A* **1998**, *102*, 280–284.

Scheme 2

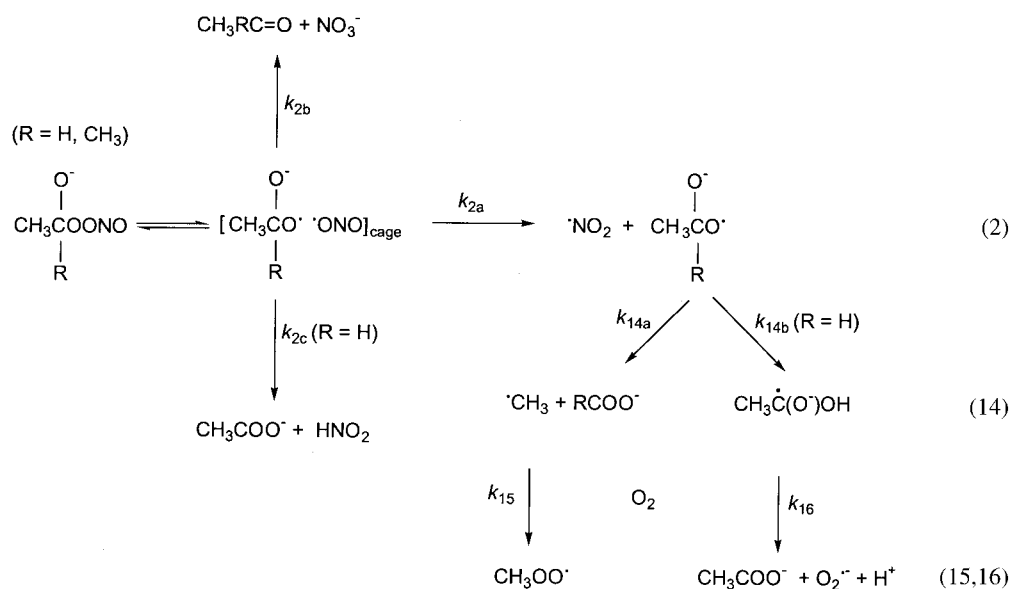


Table 4. Summary of All the Rate Constants Included in Scheme 1, and Which Are Derived from the Present Study

	acetone	acetaldehyde
$K_1 k_2, \text{M}^{-1} \text{s}^{-1}$	0.014 ± 0.003	115 ± 23
$K_1 k_{\text{H}_2\text{O}}, \text{M}^{-1} \text{s}^{-1}$	1.15 ± 0.02	$(1.27 \pm 0.04) \times 10^3$
$k_3/k_{\text{OH}}, \text{M}$	$(3.3 \pm 0.2) \times 10^{-4}$	$(7.1 \pm 0.8) \times 10^{-4}$
$k_1, \text{M}^{-1} \text{s}^{-1}$	116 ± 7	$(5.8 \pm 0.4) \times 10^4$
$k_{-1}/k_{\text{HA}}, \text{M}$	0.72 ± 0.08	0.89 ± 0.11
$k_{\text{H}_2\text{O}}/k_2$	82 ± 24	11 ± 3
k_{-1}/k_2	$(8.3 \pm 3.5) \times 10^3$	504 ± 170
$k_{-1}/k_{\text{H}_2\text{O}}$	101 ± 8	46 ± 2
$k_{\text{HA}}/k_{\text{H}_2\text{O}}, \text{M}^{-1}$	140 ± 30	52 ± 10

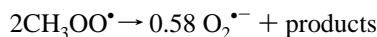
Assuming that $k_{\text{OH}} \approx 3 \times 10^9 \text{M}^{-1} \text{s}^{-1}$ (deprotonation) and $k_{\text{HA}} \approx 3 \times 10^9 \text{M}^{-1} \text{s}^{-1}$ (HA being NH_4^+), the following are obtained:

k_{-1}, s^{-1}	$\sim 2 \times 10^9$	$\sim 3 \times 10^9$
K_1, M^{-1}	$\sim 6 \times 10^{-8}$	$\sim 2 \times 10^{-5}$
k_3, s^{-1}	$\sim 1 \times 10^6$	$\sim 2 \times 10^6$
k_2, s^{-1}	$\sim 3 \times 10^5$	$\sim 5 \times 10^6$
$k_{\text{H}_2\text{O}}, \text{s}^{-1}$	$\sim 2 \times 10^7$	$\sim 6 \times 10^7$
$\text{p}K_{\text{a}}(\text{adduct})$	~ 11.8	~ 12.3

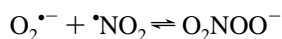
that can be obtained experimentally, are presented in Table 4. As far as the other rate constants are concerned, our experiments can disclose only ratios between them, the latter being also compiled in Table 4. However, as we shall discuss forthwith, one can arrive at very reasonable absolute rate constants, once certain plausible assumptions are made.

The Mode of Homolysis and the Fate of the Free Radicals during the Decomposition of the Carbonyl-OONO Adducts. The mechanism of decomposition of $\text{CH}_3\text{RC}(\text{O}^-)(\text{ONOO})$ (R = H, CH_3) is assumed to take place via reactions 2 and 14–21 (reactions 14–16 are shown in Scheme 2). A similar sequence of reactions is assumed for the protonated form of the adduct, where reaction 2 is replaced by reaction 3. We recall that $k_{\text{d}} \approx K_1 \alpha k_{\text{H}_2\text{O}} + K_1 k_2$. In the case of acetone, we can calculate from this equation using values in Table 4 that, at $\text{pH} \geq 13.4$, more than 90% of the products derive from the basic channel, i.e., reaction 2, while below $\text{pH} 11.4$ more than 90% of the products are provided by the acidic channel, i.e., reaction 3. The corresponding limiting pH values for acetaldehyde are 12.8 and 10.2, respectively. It is these product-determining pH regions

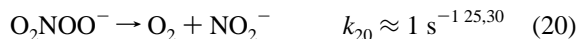
that we shall denote by “high” or “low” pH in the following discussion.



$$2k_{17} = 7.3 \times 10^8 \text{M}^{-1} \text{s}^{-1} \quad (17)$$

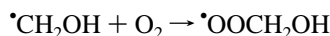
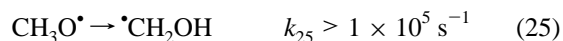
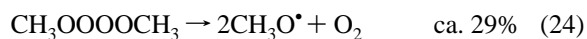
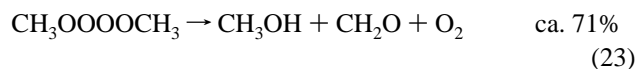


$$k_{19} = 4.5 \times 10^9 \text{M}^{-1} \text{s}^{-1.3}, k_{-19} \approx 1 \text{s}^{-1.25} \quad (19)$$

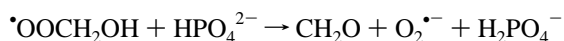


$$2k_{21} = 1.3 \times 10^8 \text{M}^{-1} \text{s}^{-1.31} \quad (21)$$

The formation of $\text{O}_2^{\bullet -}$ during recombination of $\text{CH}_3\text{OO}^\bullet$ is thought to occur according to the following mechanism:



$$k_{26} = 4.2 \times 10^9 \text{M}^{-1} \text{s}^{-1} \quad (26)$$



$$k_{27} \approx 2 \times 10^6 \text{M}^{-1} \text{s}^{-1} \quad (27)$$

According to the mechanism described by reactions 22–27, the difference between the yields of CH_2O and CH_3OH per $[\text{CH}_3\text{OO}^\bullet]_0$ should be similar to the $\text{O}_2^{\bullet -}$ yield, i.e., ca. 29%. This was indeed found to be the case.³²

Concerning the reaction scheme for adduct homolysis, i.e., reactions, 2, 14, 15, and 16 (Scheme 2), some comments are in

order. From the geminate pair that is formed by homolysis of the adduct, a small part is released as free radicals (k_{2a}). The remainder collapses to molecular products in the solvent cage. Process 2b is the predominant cage collapse with acetaldehyde and the only cage process with acetone. This is reflected by the very high yields of NO_3^- in all carbonyl/ONOO- systems.^{13–16} Process 2b is probably initiated by N–O coupling to yield a short-lived α -hydroxyalkyl nitrate, followed by rapid heterolysis resulting in nitrate and the initial carbonyl compound. Based on the significantly higher yield of acetate as compared to that of $\text{O}_2^{\bullet-}$ in the case of acetaldehyde,^{4,14} reaction 2c, which is an in-cage hydrogen atom transfer, has been suggested to occur.⁴ Once the free radicals have diffused out of the solvent cage, several processes ensue. Reaction 14a, i.e., β -scission,³³ can take place in the case of acetone and acetaldehyde, whereas reaction 14b, i.e., 1,2-H atom shift,³⁴ occurs only in the case of acetaldehyde.

We found above that the reaction of ONOO⁻ with acetone yielded about 4% $\text{O}_2^{\bullet-}$ of the initial concentration of ONOO⁻, where only about 1% was formed relatively fast, at the same rate as ONOO⁻ disappeared. We suggest that the fast formation of about 1% $\text{O}_2^{\bullet-}$ is due to the self-decomposition of $\text{CH}_3\text{OO}^\bullet$ during the lifetime of ONOO⁻, whereas the other 3% is attributed to the self-decomposition of $\text{CH}_3\text{OO}^\bullet$ formed slowly via the homolysis of CH_3OONO_2 (reaction –18), after all ONOO⁻ has been consumed. Since the self-recombination of $\text{CH}_3\text{OO}^\bullet$ was shown to yield about 29% $\text{O}_2^{\bullet-}$, and as the total $\text{O}_2^{\bullet-}$ yield from the acetone-ONOO⁻ reaction is ca. 4%, we calculate that the yield of $\text{CH}_3\text{OO}^\bullet$ formed during ONOO⁻ decomposition by acetone is $4/0.29 \approx 14\%$ of the initial concentration of ONOO⁻. This implies that about 14% of the geminate radical pairs formed during homolysis of the peroxidic adduct escape from the solvent cage, given that the precursor of $\text{CH}_3\text{OO}^\bullet$ is the $(\text{CH}_3)_2\text{C}(\text{OH})\text{O}^\bullet$ radical. Furthermore, since 3% out of the total 4% $\text{O}_2^{\bullet-}$ was formed via the slow homolysis of CH_3OONO_2 , it follows that about 75% of the initially formed $\text{CH}_3\text{OO}^\bullet$ recombined with $\bullet\text{NO}_2$ and only about 25% underwent self-recombination. This can be shown³⁵ to imply that $k_{18}/k_{17} \approx 4$, whence $k_{18} \approx 1.5 \times 10^9 \text{ M}^{-1} \text{ s}^{-1}$ follows. The rate constant for the slow formation of $\text{O}_2^{\bullet-}$ was measured to be 0.015 s^{-1} . Assuming the steady-state approximation for $[\text{CH}_3\text{OO}^\bullet]$ and $[\bullet\text{NO}_2]$ formed in reaction –18 and consumed in reactions 17, 18, and 21, we derive the latter rate constant to be $2k_{17}k_{-18}/\{2k_{17} + k_{18}(k_{17}/k_{21})^{1/2}\} \approx (K_{18})^{-1}(2k_{17}2k_{21})^{1/2}$. Thus, $(K_{18})^{-1} \approx 4.9 \times 10^{-11} \text{ M}$ and $k_{-18} \approx 0.07 \text{ s}^{-1}$, where the former value is close to that of the equilibrium constant of dissociation of HOONO_2 into HO_2^\bullet and $\bullet\text{NO}_2$, which is $1.4 \times 10^{-11} \text{ M}$.²⁸

The rate constant for the oxidation of ferrocyanide by $\text{CH}_3\text{-OO}^\bullet$ ($k = 7.1 \times 10^3 \text{ M}^{-1} \text{ s}^{-1}$) is much lower than that for

oxidation by $\bullet\text{NO}_2$ ($k = 4.3 \times 10^6 \text{ M}^{-1} \text{ s}^{-1}$).³⁶ Therefore, while 0.1 M ferrocyanide is sufficient to reduce all $\bullet\text{NO}_2$, it falls somewhat short of capturing $\text{CH}_3\text{OO}^\bullet$ quantitatively. The data in Table 3 reveal that the yield of the radicals escaping the cage in the acetone system is above 14%. On the other hand, a radical yield of 15% was obtained when we simulated the yield of $\text{Fe}(\text{CN})_6^{3-}$ with known rate constants in the presence of 1 M $\text{Fe}(\text{CN})_6^{4-}$ and this yield was unaffected by a further increase in $[\text{Fe}(\text{CN})_6^{4-}]$. Thus, the combined $\text{Fe}(\text{CN})_6^{4-}$ and TNM experiments are consistent with a free radical yield of 14–15% at low pH.

As mentioned above, the radical yield at high pH was not measurable. However, the yield of the free radicals should be equal to the acetate yield (reaction 14a, where $\text{R} = \text{CH}_3$), which we determined to be $13 \pm 2\%$ at $\text{pH} > 14$. In conclusion, in the reaction of ONOO⁻ with acetone, the free radical yields at low and high pH are similar and amount to 13–15%.

The reaction of ONOO⁻ with acetaldehyde formed $8.7 \pm 0.4\%$ O_2NOO^- of the initial ONOO⁻ at low pH, which approximates the yield of $\text{O}_2^{\bullet-}$ in this system and is in agreement with the previously reported yield of $\text{O}_2^{\bullet-}$ determined by use of TNM.⁴ The yield of ferricyanide at low pH and in the presence of 0.1 M ferrocyanide is ca. 20% (Table 3). While this concentration of ferrocyanide is sufficient to scavenge the excess of $\bullet\text{NO}_2$, it is not sufficient completely to prevent the recombination of $\bullet\text{NO}_2$ with $\text{O}_2^{\bullet-}$ and to scavenge all $\text{CH}_3\text{OO}^\bullet$. We therefore used our suggested model (reactions 2 or 3, 14–21) to simulate the yield of ferricyanide both at low and high pH, taking into account 8.7% and 10.9% yields of $\text{O}_2^{\bullet-}$ at low and high pH, respectively. We also included in this model the oxidation of ferrocyanide by $\text{CH}_3\text{OO}^\bullet$ and $\bullet\text{NO}_2$ and the reduction of $\text{Fe}(\text{CN})_6^{3-}$ by $\text{O}_2^{\bullet-}$, i.e., $k = 6.9 \times 10^3 \text{ M}^{-1} \text{ s}^{-1}$ at $I = 0.2 \text{ M}$.³⁷ The model fits the experimental results (Table 3) assuming about 16% radical yield and 47% β -scission at low pH, and about 17% radical yield and 37% β -scission at high pH. The low pH results are in fair agreement with previous yields obtained at 37 °C, where the total radical yield was ca. 20%, about half of it being $\bullet\text{CH}_3$ radicals formed during β -scission.¹⁴

The Properties of the Carbonyl-OONO Adduct. Two reasonable assumptions can be made for molecules of the size of the carbonyl-OONO adducts: (i) The rate constant of their deprotonation by OH^- is constant and diffusion-controlled, with $k_{\text{OH}} \approx 3 \times 10^9 \text{ M}^{-1} \text{ s}^{-1}$, and this value could hardly be wrong by more than a factor of 2 or so. (ii) The rate of protonation of the adduct anions by NH_4^+ is diffusion-controlled. As the rate constant of proton self-exchange in the reaction $\text{NH}_3 + \text{NH}_4^+ \rightleftharpoons \text{NH}_4^+ + \text{NH}_3$ is as high as $10^9 \text{ M}^{-1} \text{ s}^{-1}$,³⁸ and the $\text{p}K_a$'s of the adducts are higher than $\text{p}K_a(\text{NH}_4^+)$ (vide infra), k_{HA} in the case of NH_4^+ should lie between 10^9 and $10^{10} \text{ M}^{-1} \text{ s}^{-1}$. We therefore settle for the geometric mean of $3 \times 10^9 \text{ M}^{-1} \text{ s}^{-1}$, which should be accurate within better than a factor of 2. With these two assumed rate constants, all the other rate constants can be unravelled (Table 4). The highest rate constant obtained is for the reverse of reaction 1, i.e., $k_{-1} > 10^9 \text{ s}^{-1}$, implying a lifetime below 1 ns for the carbonyl-OONO adduct. Similar short lifetimes have been reported for the tetrahedral intermedi-

(30) Logager, T.; Sehested, K. *J. Phys. Chem.* **1993**, *97*, 10047–10052.

(31) Graetzel, M.; Henglein, A.; Lilie, J.; Beck, G. *Ber. Bunsen-Ges. Phys. Chem.* **1969**, *73*, 646–653.

(32) Schuchman, H.-P.; von Sonntag, C. *Z. Naturforsch.* **1984**, *39B*, 217–222.

(33) Walling, C.; Wagner, P. J. K. *J. Am. Chem. Soc.* **1964**, *86*, 3368–3375.

(34) Gilbert, B. C.; Holmes, R. G. G.; Laue, H. A. H.; Norman, R. O. C. *J. Chem. Soc., Perkin Trans. 2.* **1976**, 1047–1052.

(35) During the lifetime of ONOO⁻ one can neglect reactions –18 and 21 in comparison to 17 and 18. One then obtains for the consumption of $\text{CH}_3\text{-OO}^\bullet$ and $\bullet\text{NO}_2$ the simplified equations $-\text{d}[\text{CH}_3\text{OO}^\bullet]/\text{d}t = 2k_{17}[\text{CH}_3\text{OO}^\bullet]^2 + k_{18}[\text{CH}_3\text{OO}^\bullet][\bullet\text{NO}_2]$ and $-\text{d}[\bullet\text{NO}_2]/\text{d}t = k_{18}[\text{CH}_3\text{OO}^\bullet][\bullet\text{NO}_2]$. This system of coupled differential equations is exactly solvable, and with the initial condition $[\text{CH}_3\text{OO}^\bullet]_0 = [\bullet\text{NO}_2]_0$ one obtains $\ln F = \{r/(1-r)\} \ln r$, where F is the fraction of $\text{CH}_3\text{OO}^\bullet$ consumed in reaction 17, in the event $\approx 1/4$, and r is defined as $k_{18}/2k_{17}$. Thus, $r \approx 2$ and $k_{18}/k_{17} \approx 4$ is calculated.

(36) Ottolenghi, M.; Rabani, J. *J. Phys. Chem.* **1968**, *72*, 593–598.

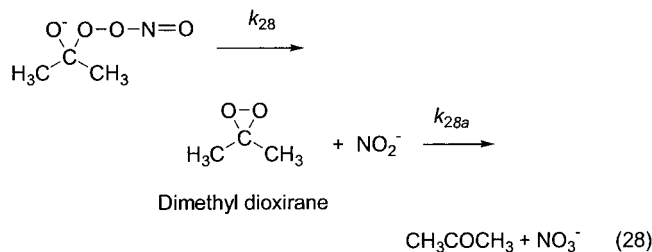
(37) Bradic, Z.; Wilkins, R. G. *J. Am. Chem. Soc.* **1984**, *106*, 2236–2239.

(38) Meiboom, S.; Loewenstein, A.; Alexander, S. *J. Chem. Phys.* **1958**, *29*, 969–970.

ates formed during alkaline hydrolysis of benzoate esters.^{17a} As can be seen from Table 4, the rate constants for protonation of the adduct anions by H₂O, *k*_{H₂O}, are well below 10⁸ s⁻¹. As these values are significantly lower than *k*₋₁, it follows that equilibrium 1 is faster established than the protonation equilibrium of the adduct. Combination of *k*_{H₂O} with *k*_{OH} enabled us to estimate the p*K*_a values of the adducts, which are also tabulated in Table 4.

The most important results in this work are the derived rate constants for the homolysis of the carbonyl-OONO adducts. Both adducts homolyze with rate constants of around 10⁶ s⁻¹, and these values vary little when the adducts are deprotonated. This suggests that the O–O bond strengths in the adducts are hardly affected by their protonation states. The short lifetime of the adducts implies that, while they may form in biological systems, they cannot act directly as oxidants. Thus, any biological damage in such systems must be ascribed to the free radicals that form rapidly as a result of adduct homolysis. We note that the lifetime of the carbonyl-OONO adducts is shorter by about 6 orders of magnitude than that of ONOOH. This is in keeping with the fact that the strength of the O–O bond decreases by 6–8 kcal/mol upon replacing H with an alkyl group in a hydroperoxide.³⁹ This finding can be rationalized in terms of hyperconjugative stabilization of the alkoxy radical as compared to the unstabilized hydroxyl radical.

Does the Reaction of Acetone with ONOO⁻ Form Dioxirane? It has been previously suggested that the reaction of ketones with ONOO⁻ forms ketone-OONO adducts, which decompose mainly to form dioxirane as intermediates via a formal two-electron oxidation (reaction 28).¹⁵ In the present



work we have demonstrated that the decomposition of the acetone-OONO adduct proceeds via homolysis in both reactions 2 and 3, but the question remains whether dioxirane formation can also occur in this system. If ONOO⁻ decomposed mainly via equilibrium 1 followed by reaction 28, this would mean that *k*₂₈ would make up the major part of *k*₂, i.e., reaction 28 would constitute a larger part of channel 2 than homolysis. On the other hand, as we discussed above, at low pH it is predominantly channel 3, i.e., the neutral adduct, that provides the end-products, and, according to the above scheme, this channel cannot yield dioxirane. Indeed, from the finding that the rate constant of decay of ONOO⁻ at low pH, even in the absence of a buffer, is as high as 1.15 M⁻¹ s⁻¹, i.e., higher by about 2 orders of magnitude than at high pH (0.014 M⁻¹ s⁻¹), we conclude that below ca. pH 10 less than 1% of ONOO⁻ can yield dioxirane.

In principle, dioxirane might be formed efficiently at high pH. However, as will be shown below, this can be all but

precluded on kinetic grounds. In ref 19, a linear free energy relationship was derived between the p*K*_a of the conjugate acid of a nucleophile and the p*K*_a of the corresponding adduct to a carbonyl group. This implies that one can set

$$\frac{\text{p}K_a((\text{CH}_3)_2\text{C}(\text{OOH})\text{OH}) - \text{p}K_a((\text{CH}_3)_2(\text{OONO})\text{OH})}{\text{p}K_a(\text{CH}_3\text{C}(\text{OH})_2) - \text{p}K_a((\text{CH}_3)_2(\text{OONO})\text{OH})} \approx \frac{\text{p}K_a(\text{H}_2\text{O}_2) - \text{p}K_a(\text{ONOOH})}{\text{p}K_a(\text{H}_2\text{O}) - \text{p}K_a(\text{ONOOH})}$$

From p*K*_a((CH₃)₂(OONO)OH) ≈ 11.8, p*K*_a((CH₃)₂C(OH)₂) = 14.5,²² p*K*_a(H₂O) = 15.7, p*K*_a(ONOOH) = 6.6, and p*K*_a(H₂O₂) = 11.7, we estimate p*K*_a((CH₃)₂C(OOH)OH) ≈ 13.3.⁴⁰

The equilibrium constant of reaction 29 was reported to be 0.086 M⁻¹.⁴¹

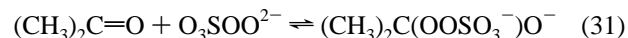


and using p*K*_a((CH₃)₂C(OOH)OH) ≈ 13.3, we calculate *K*₃₀ ≈ 2 × 10⁻³ M⁻¹.



Significantly, log *K*₃₀ – log *K*₁ ≈ 4.5 is close to the difference between p*K*_a(H₂O₂) and p*K*_a(ONOOH), i.e., 5.1.

The kinetics of dioxirane formation was studied with SO₅²⁻ as the nucleophile,⁴² and from published data one calculates *K*₃₁*k*₃₂ ≈ 0.1 M⁻¹ s⁻¹.



Since SO₅²⁻ is also a hydroperoxide anion and p*K*_a(HSO₅⁻) = 9.4, we can predict from the above relationship that log *K*₃₁ ≈ log *K*₁ + 2.5. Furthermore, since p*K*_a(HSO₄⁻) = 2.0 is lower by about 1 unit than p*K*_a(HNO₂) = 3.1, *k*₂₈ should be smaller than *k*₃₂. From these data we arrive at the conclusion that *K*₁*k*₂₈ should be around 10⁻⁴ M⁻¹ s⁻¹. However, as the experimental rate constant of ONOO⁻ decay in the presence of acetone at high pH is 0.014 M⁻¹ s⁻¹, we conclude that *k*₂₈ makes up less than 1% of *k*₂, and therefore not even at high pH can ONOO⁻ produce more than 1% dioxirane with acetone.

Actually, even without carrying through this analysis, the finding that the free radical yields are almost the same at low and high pH strongly suggests similar mechanisms in these two pH regions. Therefore, since the low-pH channel, reaction 3, can only involve homolysis, so should the high-pH channel, reaction 2. This is further supported by the similar values derived for rate constants *k*₂ and *k*₃.

In view of the fact that several hydroperoxides, such as peroxy acids and Caro's acid, produce efficiently dioxiranes⁴³ from ketones, one might wonder why ONOO⁻ should be an exception. Clearly, the reason is the extremely weak O–O bond in carbonyl-OONO adducts. This opens up O–O bond homolysis as a new channel of decomposition, which competes efficiently

(40) This p*K*_a refers to deprotonation of the OH group. As in reality the OOH group is more acidic than the OH group and thus deprotonates at lower pH, this p*K*_a ≈ 13.3 should be considered as a microscopic p*K*_a.

(41) Sauer, M. C. V.; Edwards, J. O. *J. Phys. Chem.* **1971**, *75*, 3004–3011.

(42) Lange, A.; Brauer, H.-D. *J. Chem. Soc., Perkin Trans. 2* **1996**, 805–811.

(43) Murray, R. W. *Chem. Rev.* **1989**, *89*, 1187–1201.

(39) Cremer, D. In *The Chemistry of Peroxides*; Patai, S., Ed.; John Wiley: New York, 1983; pp 1–84.

with the formation of dioxirane. For most other carbonyl-hydroperoxide adducts the O–O bond is sufficiently strong to bar homolysis as a competitor to heterolysis. Finally, although we have provided strong evidence against dioxirane formation in the acetone system, we cannot exclude it in the case of more activated ketones.¹⁵ In ref 15, dioxirane formation was implied on the grounds that certain alkenes were epoxidized in the ketone-ONOO⁻ system with similar stereoselectivity as in the ketone/SO₅²⁻ system, and in the latter dioxirane formation is known to occur. We note, however, that in these activated ketone-ONOO⁻ systems, relatively long-lived alkyl- or acyl-peroxynitrates are likely to form after radical homolysis (see the discussion about CH₃OONO₂, above). It is conceivable that these highly activated peroxides may exhibit similar epoxidation selectivity vis-à-vis alkenes as the well-investigated dioxiranes. At any rate, these points are in need of additional investigation before the matter can be considered settled.

Conclusions

Peroxynitrite is involved in rapid nucleophilic addition equilibria with both acetaldehyde and acetone, whereby tetrahedral adduct anions are formed. The equilibria are strongly

shifted to the reactant side with both carbonyl compounds. The adduct anions also undergo protonation by water and added buffers. Both the anionic and the neutral adducts undergo homolysis along the weak O–O bond. The rate constant for this process was derived to be close to 10⁶ s⁻¹ for all the adducts, varying by no more than about 1 order of magnitude, when changing the carbonyl precursor or the protonation state of the adduct. The short lifetime of the adducts prevents them from acting as biological oxidants. The homolysis yielded ca. 15% free radicals, while the remainder formed molecular products, produced in the solvent cage. Several rate constants and equilibrium constants were extracted from the data. Dioxirane formation in the acetone system was shown to be insignificant.

Acknowledgment. G.M. acknowledges the Swedish Science Council for financial support. We are also grateful to Mr. Johan Andersson and Prof. Anna-Karin Borg for their expert help in performing the GC experiments. The authors have appreciated some useful comments from Dr. Sergei Lymar as well as from the three reviewers of this manuscript.

JA011799X